Steel Case Hardening Using Deformational cutting

Nikolai Zubkov, Victor Poptsov*, Sergey Vasiliev and Andre DL Batako

Nikolai Zubkov

Affiliation: Bauman Moscow State Technical University
Mailing address: 2-ya Baumanskaya str. 5, 105005 Moscow, Russia
E-mail: zoubkovn@bmstu.ru

Victor Poptsov *
**Corresponding author*
Affiliation: Bauman Moscow State Technical University
Mailing address: 2-ya Baumanskaya str. 5, 105005 Moscow, Russia
E-mail: poptsov-v.v@yandex.ru
Cell phone: +79166163876

Sergey Vasiliev
Affiliation: Bauman Moscow State Technical University
Mailing address: 2-ya Baumanskaya str. 5, 105005 Moscow, Russia
E-mail: sergv@bmstu.ru

Andre DL Batako
Affiliation: Liverpool John Moores University, United Kingdom
Mailing address: Liverpool John Moores University, Byrom Street, Liverpool, L3 3AF, United Kingdom
E-mail: a.d.batako@ljmu.ac.uk

ASME Trans, J. Manuf. Sci. Eng 140(6), 061013 (Apr 02, 2018) (8 pages) Paper No: MANU-17-1546; doi: 10.1115/1.4039382 History: Received September 01, 2017; Accept February 10, 2018

ABSTRACT

This article describes some fundamental principles, specific features and the technological capabilities of a new method of quenching steel surface by turning without separation of chips. The underlying process of this method is a deformational cutting which is based on the undercutting and deformation of surface layers that remain attached to the workpiece. The

energy released in the area of deformational cutting is used to heat the undercut layer up to the temperatures of structural and phase transformation of workpiece material. This type of process results into a hardened structure formed at the surface which consists of inclined thin undercut layers tightly packed and stuck (glued) together and form a single solid body. The resulting hardened structures achieved in steels workpieces are presented in the article. The samples hardened by deformational cutting showed a higher wear resistance compared to samples with traditional quenching. This paper also describes an estimation of the thermo-physical parameters of the deformational cutting process.

KEYWORDS

Case hardening, surface quenching, phase transformation, wear resistance, deformational cutting, heating rate.

NOMENCLATURE

a_p - depth of cut (mm),
b - interfin gap width (mm),
C_p - specific heat capacity (J/(kg·^{o}C)),
d- the length of the contact zone (mm),
f - feed per revolution (fin pitch) (mm),
G - mass flow rate of metal passing through the treatment area (g/s),
l_f - path length of friction (mm),
K_r, - side cutting edge angle (◦),
N - power which is released in the cutting zone (W),
P_z - tangential cutting force component (N),
p_{DC} - specific cutting force (Pa),
q - volume flow rate of metal passing through the DC zone (cm3/s),
Q - energy to volume ratio (kJ/cm3),
t - time, during which the metal remains in the heating area (s),
V - cutting speed (m/s),
V_{heat} - rate of heating (◦C/s),
ρ - specific weight (kg/m^3),
φ_e - end cutting edge angle (◦),
W – wear rate of the sample (m^3/(m•N)
Δh - volume loss during wear after one hour of testing (mm^3).
F_n - load applied during tribological tests (N)

1. STATE OF ART

1.1 Machining for surface quenching

Surface quenching is one of the efficient and cost-effective methods of increasing hardness and wear resistance of machine parts. In machines and mechanisms operating under high contact load with relative speed, abrasive wear is a real challenge for keeping parts in their original shape and performance [1]. There exist a number of surface quenching technologies, most of which require specialized equipment to achieve structural and phase transformations during quenching of steels [2]. A relatively new method of surface hardening is a direct quenching workpiece machine tools without addition equipment. Here, the temperatures required for quenching are reached in the cutting process due to plastic deformation and friction in the contact area between the tool and workpiece. The combined effect of severe deformation, high local temperatures, and rapid quenching rates causes the machined surface to undergo both physical and metallurgical transformations [3].

Quench hardening by machining can be undertaken with single point cutting tools that have a well-defined geometry of the cutting edges and grinding process. The effect of increasing surface hardness in turning process was underlined by Guo et al. [4]. Naik et al. [5] used a cutting tool with a zero-clearance angle to enhance friction between workpiece and tool. Kundraket et al [6] also observed hardening of surface using cutters with negative rake angles in turning.

Quench-grinding is a process where the grind wheel is driven into the workpiece in a way that the heat generated within the cutting zone is used for heating and hardening the surface layer of the part, which is the only process similar to the DC quenching presented here. Forced grinding can be applied to steels with over 0.3% of carbon to achieve Quench-

grinding. This mode of grinding has a number of advantages compared to hardening based on quench-turning. Here, the thickness of the hardened layer relative to the removed defective layer is 0.3-0.5 mm, and the heat affected zone reaches up 2 mm, with a surface hardness up to 50-60 HRC [3,7]. The depth of cut in this force grinding ranges from 0.2 mm to 1.2 mm, and the longitudinal feed of the grinding wheel can be from 0.3 to 1.2 m/min. In this process, the application of cooling fluids is not of importance since cooling is achieved by heat dissipation into the underlying cold workpiece layers [8]. This innovative process of force-grind hardening is developing rapidly, and DMG/Mori Seiki has introduced CNC grinding machines that provide additional quenching operation using specialised grinding wheels. The productivity of grind-hardening is about 4-15 sec/sq in (0.4-1.5 sm^2/s) [9] and after grind-hardening an additional process is required to remove the defective surface layer.

The work presented here employs deformational cutting (DC) method [10] to quench the surface of steel workpieces [11]. The main difference of DC quenching from other methods of hardening based on the process of cutting is that: (1) chips are not separated from the workpiece and remain attached to the surface, thus forming a special reinforced structure; (2) a uniformity of hardness throughout the hardened surface layer; (3) the possibility of generating a composite structure with alternating hard and relatively soft thin inclined layers.

The main difference between conventional cutting process and DC is that the chips are cut form one side whilst being straightened up as fins which remain as a functional part of the workpiece. A DC tool cuts and deforms the surface layers, forming a finned structure since the undercut layers are connected to the main body of the workpiece.

DC technology has a wide range of fields of application [12]. DC machining allows increasing the surface area up to twelve-fold, which is an advantage in its applications in heat exchanging processes [13]. DC is used in the manufacture of boiling surfaces and capillary

structures for heat pipes [14], along with a range of applications in electrical joints [15, 16] and slotted screen pipes [17].

1.2 Application of DC method for case hardening of steels.

It is well known that in turning chips may be heated up to the temperatures exceeding the temperatures of phase transformations in steels which may lead to hardening of chips at relevant cooling rates. In turning processes, virtually all the power of the main drive measured in kilowatts is released in the cutting zone, which has a volume of only several cubic millimetres. Consequently, the mechanical energy applied externally, is localized within the plastic deformation area and in contact zones between chip and workpiece and is converted into heat energy. The material of chip is affected by such factors as shear strain, shear strain rate, high heating rate and high cooling rate. For example, when the C45E steel (AISI 1045) is machined at a cutting speed of V=2.7 m/s, the cutting temperature may reach 1030 °C, the shear strain can reach 400 %, the shear strain rate ranges up to 10^4 s^{-1}, the heating rate shoots up 10^6 $^oC/s$. Therefore, a cooling rate of 10^3 °C/s, leads to an average normal stress of 350 MPa and an average shear stress of 250 MPa [18, 19].

During the DC process, the cooling rate of the fin material that is needed for hardening is achieved by the conductive heat transfer through the fin base into a cooler workpiece core. It is known that in heat treatment, high-frequency hardening and laser hardening can secure similar hardening cooling rates for hardening without cooling media. [20].

Figure 1 demonstrates the principle of quench turning in DC where chip separation does not occur. The DC tool 1 has one cutting edge 3 and one deforming edge 4. The deforming edge is unable to cut because it has considerable large negative rake angle (60^o in this study). The undercut layer 5 slides on the tool rake face 6 whilst, its root still keep the strong original unbroken bond with the workpiece 2. During the process of deformation in

cutting, the intensive friction occurring between the tool and deformation in zone at the deforming edge generate intensive heat into the undercut layer and after exiting the contact with the tool the heat is transferred to workpiece core. Figure 2 illustrates the actual configuration of DC quenching process of a shaft.

In performing DC to generate fins with and without gaps (tightly packed), the undercut layer may remain on the workpiece. The latter case with packed fins is depicted in Figure 3 illustrating a DC process with no gap between the fins. The dotted line denotes the contour of the tool for the previous revolution of the workpiece. The cross-section ABCD of the forthcoming fin is cut by the cutting edge BH and moves along the tool rake surface that is indicated by the arrow. The deforming edge BK determines the final position of the fin marked as BEFG.

The interfin gap b depends on the end cutting edge angle φ_e, side cutting edge angle K_r, and the feed per revolution f, which determines the pitch of the fined structure. [17].

$$b = f \cdot \sin(\varphi_e) - f \cdot \sin(K_r) = f \cdot (\sin(\varphi_e) - \sin(K_r)) \quad (1)$$

when angles φ_e and K_r are equal, the interfin gap b is theoretically and practically equal to zero. This means that DC allows obtaining densely packed structure without interfin gaps that could be considered as relatively non-porous, if one considers only the macro structure. Figure 4 provides examples of such structures for a sample steels with different feed (pitch) f.

The yield strain and friction of the undercut layer over the tool working surfaces are the sources of heat generated in the DC area. When the temperature of undercut layer exceeds the phase transition temperature and the cooling rate is high enough, the undercut layer undergoes quench hardening, which is illustrated in Figure 5a. The highest temperature in the undercut layer occurs in the contact area with the tool rake face, and, this kind of gradient

heating is used to quench fins with partially hardened section across the thickness, as depicted in Figure 5b. The alternation of fully hardened layers with softer layers is engineered to increase the functional wear resistance of sliding friction pairs.

2. EXPERIMENTAL PROCEDURE

The experimental work was undertaken using normalized ferrite-pearlite steels 20 (AISI-1020), 35 (AISI-1035) and 40Kh (AISI-5140) with workpieces of 60-80 mm in diameter. The chemical composition and initial hardness of the steels samples is presented in table 1.

Table 1. Chemical composition and hardness of steels used in the experiments.

	Steel 20 (AISI-1020) 190 HB	Steel 35 (AISI-1035) 207 HB	Steel 40Kh (AISI-5140) 190 HB
C	0.17-0.24	0.32-0.4	0.36-0.44
Si	0.17-0.37	0.17-0.37	0.17-0.37
Mn	0.35-0.65	0.5-0.8	0.5-0.8
Ni	≤ 0.25	≤0.25	≤ 0.3
S	≤ 0.04	≤0.04	≤ 0.035
P	≤ 0.04	≤0.035	≤ 0.035
Cr	≤0.25	≤0.25	0.8-1.1
Cu	≤ 0.25	≤0.25	≤ 0.3

For the machining process, a 11.0 kW lathe with maximum spindle speed of 1600 RPM was used for the DC tests. The angle on the tool side cutting edge was equal to the angle on the end cutting edge, $K_r=\varphi_e=42^o$. The cutting speed V ranged from 3 to 5 m/s, with a feed rate of f=0.05-0.4 mm/rev, and the depth of cutting was a_p=1.0-2.0 mm.

The measurements of the surface of undercutting layers were carried out using a measurement (IRTIS-2000S) with a resolution of 200 μm between two measured points at a distance of 200 millimeters from the object of measurement. The accuracy of measurement was +/- 1% of the measured range, the calibration was carried out continuously during temperature measurements between the frames embedded in the thermograph by a black body. The thermograph measurement range was from -60^{o} to + 1700 °C.

For metallographic studies and microhardness measurement, transverse cross-sections were cut from DC hardened samples using wire spark erosion machine. The cut specimens were polished, etched and prepared using standard procedures for metallographic examinations, which were carried out on the Olympus GX51. The micro hardness was automatically measured on the hardness tester EMCOTEST DuraScan 70 using Vickers indenter with a 100 g load.

The friction tests were carried out for steel 40Kh (AISI-5140) samples on the Amsler A135 friction machine. Here "disc to disc" method was used with relative slip velocity of 0.08 m/s and load of F_n=185 N. The material of the counter-face was a cemented carbide disk (92 % WC, 8 % Co) with a hardness of 87.5 HRA. Droplets of industrial bobbin oil I20A were supplied as lubricant into the friction zone. The oil had a coefficient of kinematic viscosity about 31,6 mm^2/s at 40°C, and was delivered at a rate of 4 - 6 droplets per minute. The Linear wear, relates to the radius, of the sample was measured with a dial indicator that had a resolution of 1 micron and the readings were taken at regular intervals of 1 hour during the testing. *Comparative results are given by putting side by side the performance of the samples.* Wear rate (W) for each sample was calculated using the following expression:

$$W=\Delta h/(F_n \cdot l_f), \quad (2)$$

where Δh, [mm^3] is the volume of wear loss after an hour of testing, l_f, [mm]- path length of friction.

Friction results for DC quenched samples without tempering and with low tempering (200 ^oC within 40 min) are compared with friction results for samples made from the same steel grade subjected traditional hardening with cooling in water and standard low tempering with the same process parameters.

3. **RESULTS**

The results obtained using DC machining with full quenching through fin thickness are shown in Table 2.

Table 2. Hardness of samples after DC hardening with full quenched fins.

	Feed per revolution (fin pitch), *f*, mm	Initial hardness, ($HV_{0.1}$)	Average hardness after DC quenching $HV_{0.1}$	Hardness conversion $HV_{0.1}$ to HRC	See figure
Steel 20 (AISI-1020)	0.1	190	464	46	
Steel 35 (AISI-1035)	0.05	207	650	58	6b
Steel 35 (AISI-1035)	0.15	207	670	59	6a
Steel 40Kh(AISI-5140)	0.05	190	680	59	6c
Steel 40Kh(AISI-5140)	0.1	190	760	63	

Figure 7 illustrates the distribution of hardness as a function of the depth for DC quenched steel 35 (AISI-1035) with pitch f=0.05 mm, (curve 1) alongside with the hardness distribution for laser quenched steel ASTM 4118 [21] (curve 2). Here, it is seen that the DC hardening hardness stays almost constant up to 0.5 mm in depth from the outer surface in quenched zone, whereas the hardness of laser processing linearly decreases with depth.

The speed of deformational cutting V significantly affects the structure of the hardened layer. Higher cutting speeds (about 5 m/s) generated enough flux to heat the entire thickness

of the fin up to the quenching temperature. A fully quenched fin had a hardness of 670 $HV_{0,1}$ (59 HRC) and this is shown in Figure 8a. For decreased speeds, only part of fin in direct contact with tool rake face reached the quenching temperatures. Consequently, lowering the speed resulted into a laminated structure composed of inclined layers of different hardness as shown in Figure 8b and 8c. For laminated structures with alternating hard and mote soft layers, the measured hardness was 560 $HV_{0,1}$ and 360 $HV_{0,1}$respectively. The latter hardness is representative for strain hardening under high degrees of deformation in the process of DC.

All DC process parameters such as grade of the processed material, the feed rate and tool geometry, depth of cut have a direct effect on the structure of the hardened layer. The minimum speed at which it was possible to achieve a fully hardened surface layer was 2.5 m/s.

4. ANALYSIS AND DISCUSSION

For thermal analysis of DC performance, the following process parameters were used for quenched hardening of steel 40Kh (AISI-5140): feed rate f=0.1 mm/Rev, cutting depth a_p=1.0 mm, cutting speed V=3.0 m/s. The tangential cutting force component measured with a Kisler dynamometer was P_z=700 N. The process temperature T in the cutting zone was measured with a dynamic thermocouple was T=1100 °C. In this non-standard thermocouple, the tool and the work material are the two elements of the thermocouple. The tool is electrically insulated from the tool holder thus has no electrical connection with the machine bed. The EMF generated between the tool and workpiece during cutting was measured using a high precision millivoltmeter. This is a commonly used method and can be found in text books and numerous papers, [22].

The volume flow rate of metal q passing through the DC zone was defined as:

$$q = a_p \cdot f \cdot V = 0.3cm^3 / s. \quad (3)$$

The mass flow rate of metal *G* passing through the treatment area can be expressed as:

$$G = \rho \cdot q = 2{,}36g / s\,, \quad (4)$$

where ρ=7,85·10^3 kg/m^3 – is the specific weight of steel 40Kh (AISI-5140).

The power *N* which is released in the cutting zone was calculated as:

$$N = P_z \cdot V = 2,4kW \quad (5)$$

Assuming that all the heat generated in the treatment area is used to heat the undercut layer, the fin temperature was estimated as follows:

$$T = N/\left(C_p \cdot G\right) = 1533^\circ C\,, \quad (6)$$

where C_p = 663 J/(kg·ºC) - is the specific heat capacity for the temperature range 20-1200 ºC for medium carbon low alloyed steel [23]. However, there are some discrepancies between the calculated temperature and the temperature measured using the dynamic thermocouple. This is explained by the fact that not all the heat generated in the DC zone is induced into the undercut layer. Part of this heat flows into the tool and into the surrounding environment due to convective heat transfer and radiation. Another part of the heat goes directly into the bulk of the workpiece, bypassing the undercut layer. Another art of the energy that is consumed for elastic deformations, shattering of grains (increase in interface boundaries between grains), formation of new surfaces, formation of dislocations and their motion [24], and phase transformations.

The contact time *t*, during which the cut layer remains in the heated contact zone was estimated over the contact length *d* between undercut layer and tool face and cutting speed. The contact length is the maximum length of plastic contact between undercut layer and tool face. This length is the distance between points A and E in figure 3 taking into account the

inclination of the tool face. For the processing conditions above mentioned, the contact length was d=1.2 mm. Therefore, the contact time

$$t = d/V = 4.0 \cdot 10^{-4} s \tag{7}$$

This short time (impulse), lead to a virtually instantaneous change in the phase composition of the processed material. The heating rate V_{heat} from room temperature 20^{o} to 1100 °C in the DC contact zone was estimated as:

$$V_{heat} = \Delta T/t = 2.7 \cdot 10^{6}\ K/s \tag{8}$$

The estimated heat rate in DC (eq. (8)) process exceeds the heating rate generated in laser quenching that is typically 10^6 °C /s [25]. The ratio Q of energy to material volume generated in the DC contact zone due to plastic deformations, internal and external friction was defined as:

$$Q = N/q = 8.0 kJ/cm^3 \tag{9}$$

The specific cutting force p_{DC} was defined as the ratio of the tangential force P_z of the DC to the cross section of the undercut layer and was expressed as:

$$p_{DC} = P_z/(f \cdot a_p) = 7.0 GPa \tag{10}$$

For comparison sake of the level of energies involved in DC process one can see that the density of emitted energy in DC zone exceeds the volumetric energy release in some chemical explosives which is around 4.5-7.5 kJ/sm^3 [25], alongside with the pressure in the DC contact zone is comparable to the pressures arising at explosion (< 10 GPa) [26]. Consequently, the response of the material in terms of properties and behaviour in these extreme conditions, cannot be described within the framework of conventional machining approaches. Therefore, one can postulate that the material flow undergoes a level of superplasticity which was observed at certain stages in this process in the form of quasi viscous flows along the rake face of the tool. This is illustrated in Figure 6d with some

microstructures, where it is seen that the hardening process is accompanied by extremely fast deformations that stretched the grains, similar to volcanic lava flow (see Figure 8). Equally the spitting of undercut material on the blank surface is also visible in figure 6b.

Heated layers, as in laser quenching, are cooled by heat dissipation into the main bulk of the workpiece core. Here, a thermograph (IRTIS 2200SH) with a resolution of 200 μm between two measured points at a distance of 200 millimeters from the object of measurement was used to assess thermal gradients in DC process. The accuracy of measurement was +/- 1% of the measured range, which was -60 ° C - + 1700 ° C. The cooling rate in DC quenching was assessed based on the temperature difference of the surface of undercutting layer which was 900 ^{o}C, and the surface temperature of the neighbouring fin after one full revolution of the workpiece. The recorded difference in temperature was 450°C. The workpiece rotated at 1200 RPM, taking 0.05 s per full revolution which provided a cooling rate of V_{cool}= $9.0 \cdot 10^3$ °C/s, that is far greater than 10^3 °C/s achieved in laser quenching [27].

The examination of the results in this work showed that the surface of the hardened shaft had a degree of defects, and Figure 6 depicts some of these defects at the tops of fins in the transverse sections. The fact that the defects are located at the edges of the fins makes it easy to be removed relatively simply by hard turning using PCBN or ceramic tool on the same lathe or by grinding as a separate operation.

To estimate the performance of the DC process, a shaft of 48 mm in diameter was hardened at a rate of 0.12 m per minute, achieving up to 1 mm depth of hardened layer, which is cost effective with reference to laser and conventional quenching processes. Wear resistance tests were undertaken, and Figure 9 presents the results obtained from DC hardened workpieces, where it is seen that the DC-quenching samples have 10 to 40 % higher wear-resistance compared to the samples quenched by standard hardening.

Figure 10 presents micrographs of metallographic sections of samples, illustrating bulk material along with hardened layer and worn surface (located between white lines). It is observed here, that there are no visible defects, in terms of microcracks, chipping or microstructural modifications on worn surface and in the sublayers. The microhardness of the sublayer at the depth of 0,05 mm from worn surface was identical to the average hardness of the top layer.

CONCLUSION

The investigation in to DC-quenching presented here, raised a set of questions, such as optimization of tool geometry, selection of tool material, processes involved in the phase transformations in rapid heating and cooling under extremely high rates of deformations and pressures, and study of residual stresses in the hardened layer. It was shown that DC-quenching has a set of advantages over known processes of hardening, these are:

Eradication of heat treatment equipment due to hardening in a single operation; reduction of energy consumption due high intense heat delivered at the cutting zone; high productivity; ease to integrate in production; remove unnecessary transport operations for heat treatment. With reference to grind-hardening, DC-quenching produces no waste; secures a more uniform hardness distribution across the thickness of hardened layer; the possibility to engineer laminated layered structures with different hardness.

It is seen that, this investigation has opened a new area of further research, however the following conclusions were drawn for the presented work.

1. A new method of surface hardening by deformational cutting without chips formation was developed and evaluated.
2. Within the deformational cutting, heating temperatures and cooling rates are sufficient high to induce phase transformations and quenching of the undercut layer material. The reduction of feed rate with an increase in cutting speed engender a complete hardening and a better homogeneity of the hardened layer.
3. The heating and cooling rates in DC quenching is higher than those in laser hardening. Unlike laser hardening, phase transformations in DC occur at high pressures, high degree of plastic deformation and high strain rate.
4. It has been demonstrated that it is possible to generate laminated structures with inclined layers having different hardness.
5. The adoption of DC hardening method is cost-effective with higher productivity due to the simplicity of its integration into current production systems. This new method improves efficiency of the quenching operation, allows cutting down transport operations involved in heat treatment processes, reduces energy consumption, and possible redundancy of specialized heat treatment equipment.

ACKNOWLEDGE

The authors would like to express their gratitude to the Ministry of Education and Science of Russia (Grant № 9.5617.2017/VU), the support of which has allowed conducting the research work, the results of which are presented here

REFERENCES

[1] Rajan, T.V., Sharma, C. P., and Sharma, A., 2012, Heat treatment principles and techniques, PHI Learning Pvt. Ltd., 408 p.

[2] Davis, J. R., 2002, Surface Hardening of Steels Understanding the Basics, ASM International, USA, 319 p.

[3] Guo, Y.B., and G.M. Janowski, 2004, Microstructural Characterization of White Layers by Hard Turning and Grinding, Trans. NAMRI/SME, XXXII, pp. 367–374.

[4] Guo, Y.B., and Warren, A.W., 2004, Microscale Mechanical Behaviour of the Subsurface by Finishing Processes, ASME J. Manuf. Sci. Eng., 127, pp. 333–338.

[5] Naik, S., Guo, C., Malkin, S., Viens, D.V., Pater, C.M., and Reder, S.G., 1997, Experimental Investigation of Hard Turning, 2nd Int. Mach. & Grinding Conf., Dearborn, MI, pp. 224–308.

[6] Kundrak, J., Mamalis, A.G., Gyani, K., and Bana, V., 2011, Surface layer microhardness changes with high-speed turning of hardened steels, International journal of advanced manufacturing technology 53(1): pp. 105-112.

[7] Liu, Z.Q., Ai, X., Wang, Z.H., 2006, A Comparison Study of Surface Hardening by Grinding Versus Machining, Key Engineering Materials, Vols. 304-305, pp. 156-160,

[8] Nguyen,T., Liu,M., Zhang, L., Wu, Q., and Sun, D, 2014, An Investigation of the Grinding-Hardening Induced by Traverse Cylindrical Grinding, ASME J. Manuf. Sci. Eng. 136,

[9] Hyatt, G., 2013, Integration of Heat Treatment into the Process Chain of a Mill Turn Center by Enabling External Cylindrical Grind-Hardening, Production Engineering - Research and Development (WGP Annals) 7(6), pp. 571-584.

[10] Zoubkov, N. and Ovtchinnikov, A., 1998, Method and Apparatus of Producing a Surface With Alternating Ridges and Depressions, U.S. Patent No. 5,775,187.

[11] Zubkov, N., Vasiliev, S. and Poptsov, V., 2014, The surface quench hardening method by cutting and deforming tools, Patent of RF No. 2556897, C21D 8/00. In Russian.

[12] Kukowski, R., 2003. MDT - Micro deformation technology. In: Proceedings of ASME 2003 International Mechanical Engineering Congress and Exposition Washington, DC, Nov. 2003, pp. 305–308.

[13] Thors, P., and Zoubkov, N., 2013, Method for Making Enhanced Heat Transfer Surfaces, U.S. Patent No. 8,573,022.

[14] Yakomaskin, A., Afanasiev, V., Zubkov, N. and Morskoy, D., 2013. Investigation of Heat Transfer in Evaporator of Microchannel Loop Heat Pipe. Journal of Heat Transfer 135 (10), art. no. 101006.

[15] Solovyeva, L., Zubkov, N., Lisowsky, B. and Elmoursi, A., 2012. Novel Electrical Joints Using Deformation Machining Technology Part I: Computer Modeling. IEEE Transactions on Components, Packaging, and Manufacturing Technology 2 (10), pp. 1711-1717.

[16] Solovyeva, L., Zubkov, N., Lisowsky, B. and Elmoursi, A., 2012. Novel Electrical Joints Using Deformation Machining Technology-Part II: Experimental Verification. IEEE Transactions on Components, Packaging, and Manufacturing Technology 2 (10), 1718-1722.

[17] Zubkov, N. and Sleptsov, A., 2015, Influence of Deformational Cutting Data on Parameters of Polymer Slotted Screen Pipes, ASME J. Manuf. Sci. Eng.; 138(1) 011007-011007-7.

[18] Klocke, F., 2011, Manufacturing Processes 1: Cutting, Springer-Verlag, Berlin, Germany, p.50.

[19] Chou, S.K. and Evans, C.J., 1999, White layers and thermal modeling of hard turning surfaces, Int. Journal of Machine Tools & Manufacture vol. 39, pp.1863−1881.

[20] Fortunato, A., Ascari, A., Liverani, E., Orazi, L. and Cuccolini, G., 2013, A Comprehensive Model for Laser Hardening of Carbon Steels, J. Manuf. Sci. Eng. 135(6), :061002-061002-8.

[21] Mohamad, A, 2013, Wear Performance of a Laser Surface Hardened ASTM 4118 Steel, Eng. & Tech. Journal, 17(31), pp.2335-2344.

[22] Trent, E.M, Wright, P., 2000, Metal cutting - 4th ed., Butterworth–Heinemann, USA, p.114.

[23] Chirkin, V.S., 1974, Thermal-physical Properties of Materials for Nuclear Engineering. Handbook. Atomizdat. Moscow, p. 484 (In Russian)

[24] Davim, P., 2011, Machining of Hard Materials, Springer-Verlag, London, UK, p. 211.

[25] Burakowski, T. and Wierzchon, T., 1998, Surface Engineering of Metals: Principles, Equipment, Technologies, CRC Press, NY, USA, p. 592

[26] Altgilbers, L., 2011, Explosive pulsed power,Imperial College Press, London, p. 596

[27] Majumdar, J.D. and Manna, I., 2013, Laser-Assisted Fabrication of Materials, Springer-Verlag, Berlin, Germany, 485 p.

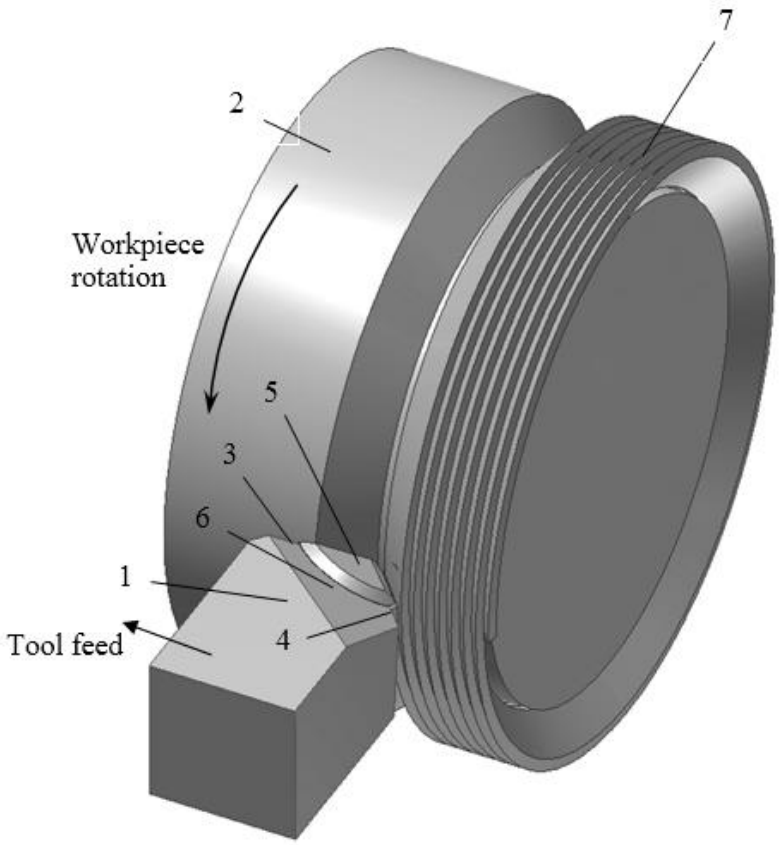

Fig. 1. Concept of DC hardening. 1 - DC tool, 2 - workpiece, 3 - cutting edge, 4 - deforming edge, 5 - undercut layer, 6 - tool rake face, 7-hardened fins.

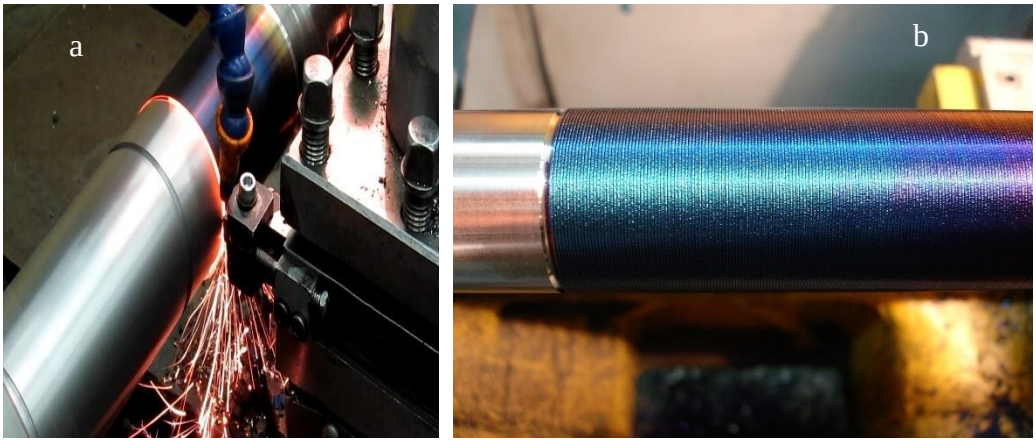

Fig. 2. Actual configuration of DC hardening process (a) and hardened of a shaft (b).

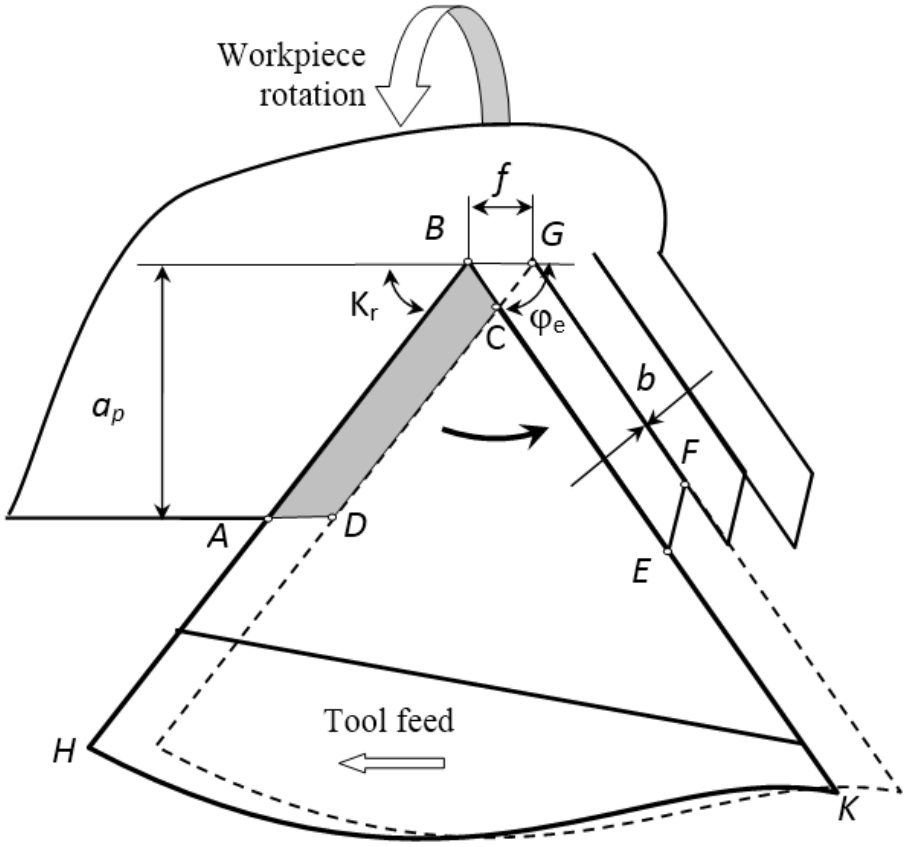

Fig. 3.DC Fin forming with zero width of interfin gap.

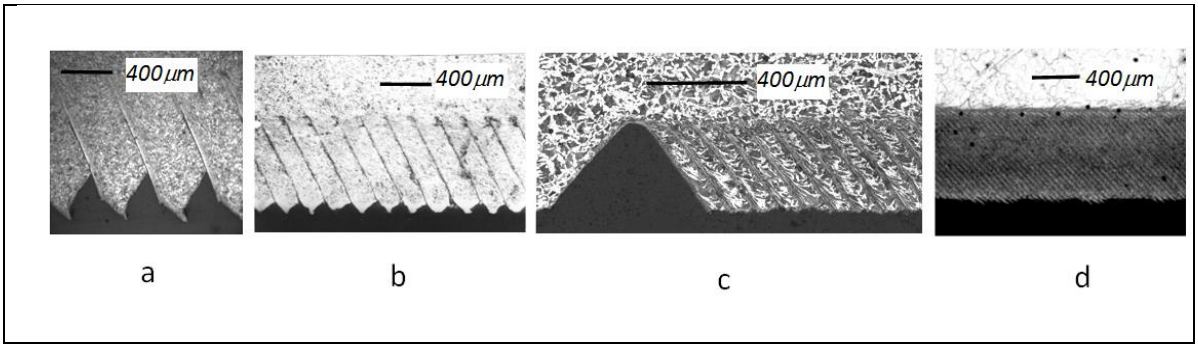

Fig. 4. Examples of deformational cutting on steels with a zero interfin gap.

a- steel 30Kh (AISI 4140), *f*=0,4 mm;

b- steel 20Kh (AISI 420), *f*=0,2 mm;

c- steel 35 (AISI 1035). *f*=0,1 mm;

d- armco-iron, *f*=0,1 mm.

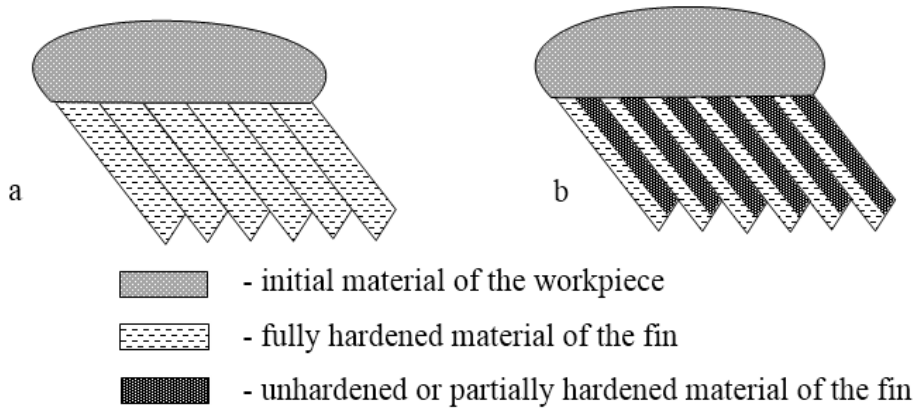

Fig. 5. Variants of structures obtained during DC quenching:

a- fully hardened fins, b – fins partially hardened over their thickness

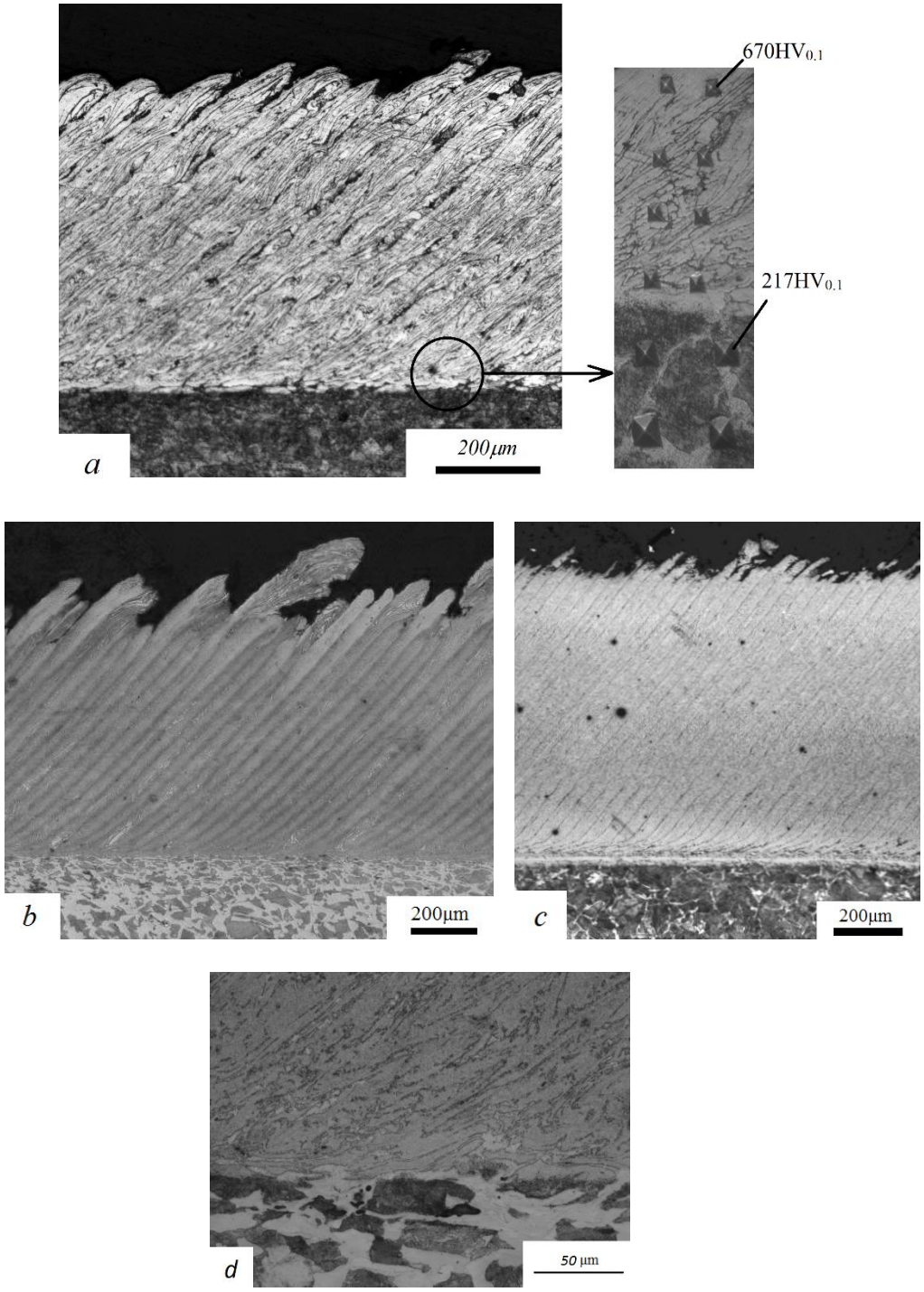

Fig. 6. Full hardening over the thickness of fins. *a*- steel 35, *f*=0.15 mm, 670 $HV_{0.1}$, *b* - steel 35(AISI-1035), *f*=0.05 mm, 650$HV_{0.1}$, *c* - steel 40Kh(AISI-5140), *f*=0.05 mm, 680$HV_{0.1}$, d - steel 35(AISI-1035), *f*=0.15 mm, 670 $HV_{0.1}$ with higher magnification.

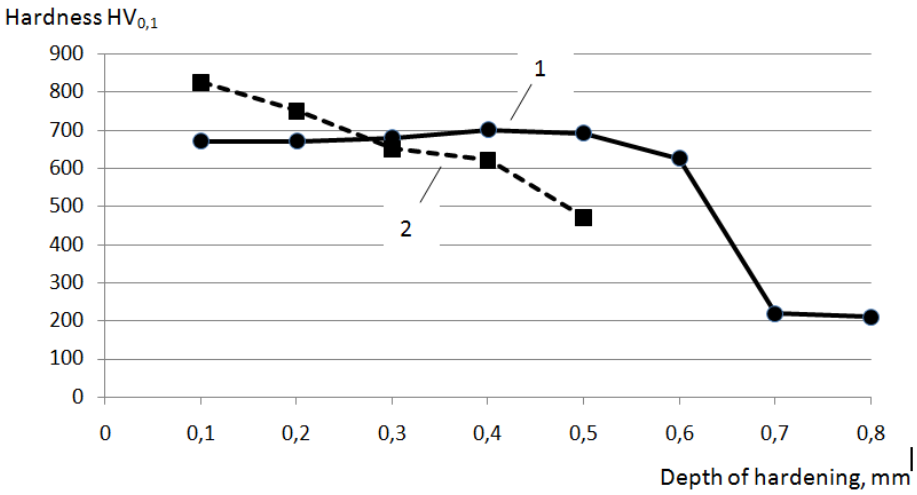

Fig. 7. Hardness distribution curves along hardening depth:
1- DC quenching; 2 laser quenching.

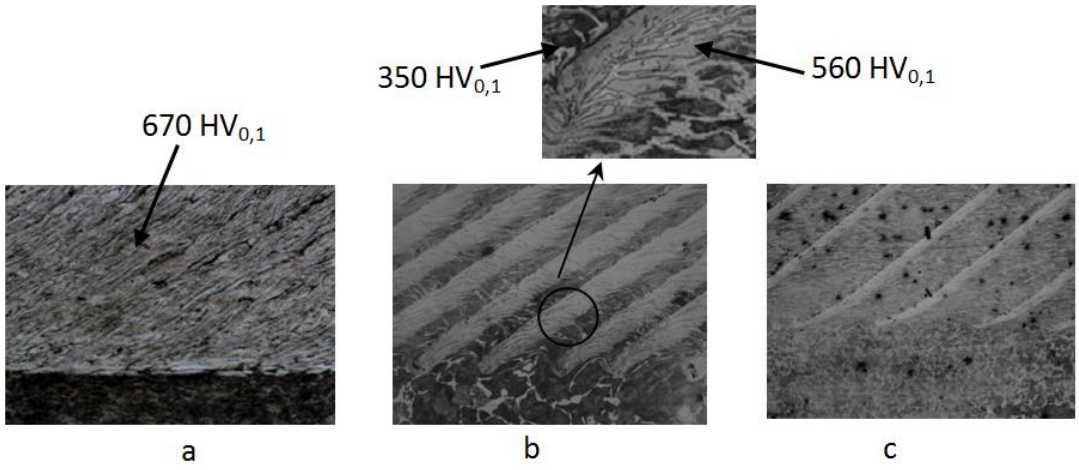

Fig. 8. Changing in the structure of hardened surface with decreasing the cutting speed. Steel 35(AISI-1035). a - *V*=4.9 m/s, quenched all fin thickness, b - *V*=3.7 m/s, quenched half a fin thickness, *c*- *V*=2.95 m/s, quenched 1/8 of fin thickness.

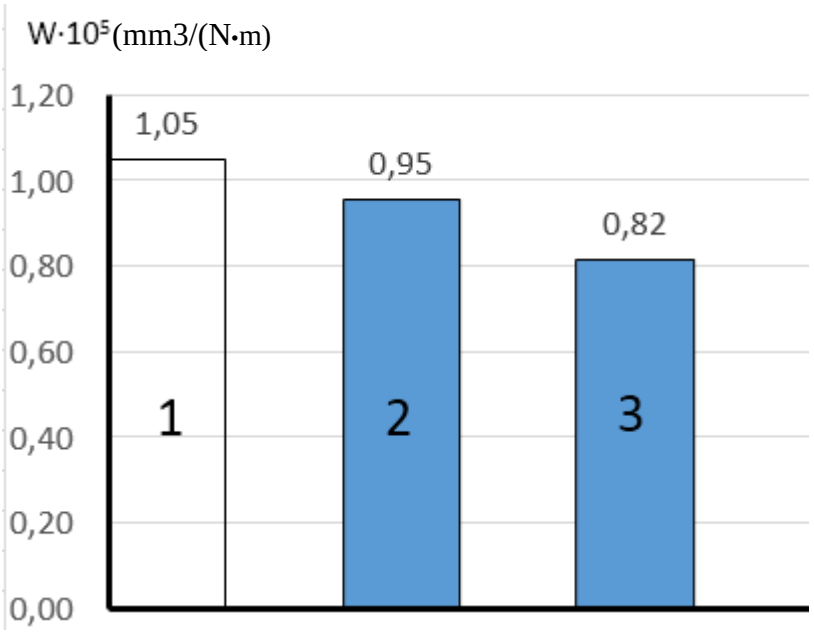

Fig. 9. Wear rate: Steel 40Kh.

1 - standard quenching (cooling in water) with low-temperature tempering (200°C, 40 min),

2 - DC quenching without tempering,

3 - DC with low-temperature tempering (at 200 °C for 40 min).

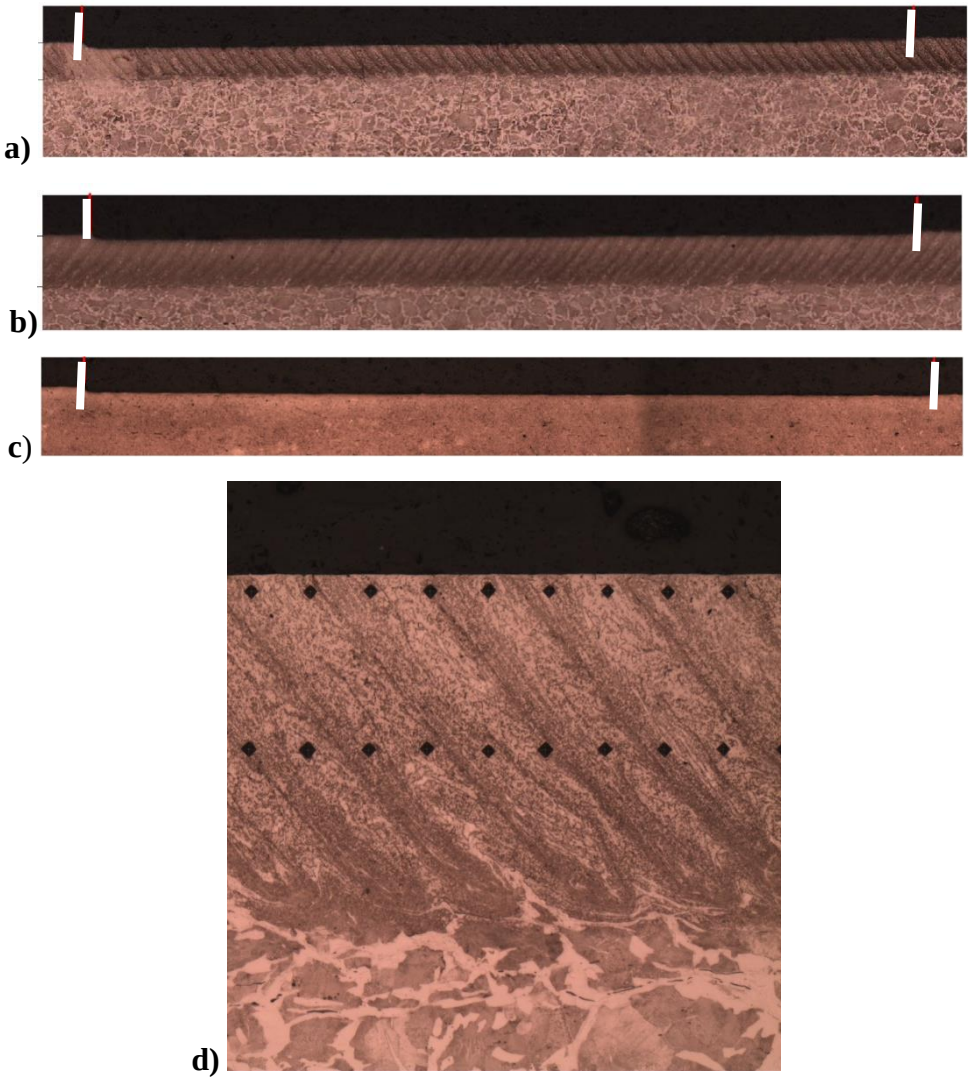

Fig. 10. Micrographs of hardened sections of 40Kh(AISI-5140) steel.

a – DC quenching without tempering (x25),

b – DC, low-temperature tempering (200 ºC, 40 min) (x25),

c – standard quenching (water cooling), low-temperature tempering (200 ºC, 40 min) (x25),

d –worn surface of "b" sample with microhardness indents (x120)